Vol 13 No 8, August 2004
1009-1963/2004/13(08)/1251-08

Chinese Physics

© 2004 Chin. Phys. Soc.
and IOP Publishing Ltd

Variation of the absorption and dispersion profiles in a ladder-four-level system

Li Yong-Fang(李永放)†, Sun Jian-Feng(孙建锋), and Niu Yue-Ping(钮月萍)

College of Physics and Information Technology, Shaanxi Normal University, Xi'an 710062, *China*

(Received 7 August 2002; revised manuscript received 30 November 2003)

A theoretical research on the variation of the absorption and dispersion profiles and population distribution of each level in a ladder-four-level system driven by two coherent fields has been made. Whether the variation occurs or not depends on the effect of quantum interference, the detuning of the upper coherent field and the separation of the two intermediate levels. A dressed-state analysis is introduced to explain the numerical results.

Keywords: quantum interference, dressed-state, absorption and dispersion profile, population distribution

PACC: 3250, 3270

1. Introduction

In resent years, quantum interference between dipole transitions of multi-level atom systems has become one of the hottest problems. Many interesting physical phenomena are ascribed to quantum interference processes, such as lasing without inversion,[1−7] enhancement of the refractive index in transparent media,[8−10] quenching of spontaneous emission,[11−13] coherent population trapping[14−18] and electro-magnetically induced transparency[19,20] etc. Zhou and Swain have studied the quantum interference between two excitation paths in V-type four-level system that gives rise to narrow resonance, gain without inversion and dark transitions.[21−23] In addition, Narducci and Scully have found that the resonance fluorescence spectrum can be controlled by the applied field.[24] Li *et al* have investigated the relationship between quantum interference and resonance fluorescence in the quasi-V-type four-level atom system.[25]

In this paper, we calculate the absorption and dispersion profiles and population distribution of each level numerically by making use of density matrix motion equations. When the quantum interference effect is small or omitted, the absorption and dispersion profiles are normal. In contrast, when the interference effect is taken into account, variation of the absorption and dispersion profiles occurs. Under certain conditions, the profiles become thoroughly inverse. In this instance, gain without inversion appears in the absorption profile. A clear analytical explanation for our numerical results is presented through a dressed-state theory.

2. Theoretical model and motion of density matrix

The model under consideration has four levels as shown in Fig.1. The transitions from the upper level $|4\rangle$ with energy $\hbar\omega_4$ to a pair of intermediate levels $|2\rangle$ with energy $\hbar\omega_2$ and $|3\rangle$ with energy $\hbar\omega_3$ are driven

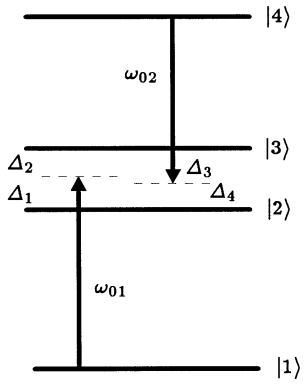


Fig.1. Schematic diagram of four-level ladder system, ω_{01}, ω_{02} are frequencies of two coherent fields, $\Delta_i (i = 1, 2, 3, 4)$ are detunings of each level.

†E-mail address: yfli@snnu.edu.cn

by a coherent field with frequency ω_{02} while the transitions from the two intermediate levels to the ground level $|1\rangle$ with energy $\hbar\omega_1$ are driven by another coherent field with frequency ω_{01}. All transitions are also coupled by vacuum modes. We assume the vacuum modes that couple $|3\rangle$ to $|1\rangle$ and $|2\rangle$, $|4\rangle$ to $|2\rangle$ and $|3\rangle$ are the same. Meanwhile, we assume that the transition from $|4\rangle$ to $|1\rangle$ is dipole forbidden.

Therefore, we can write down the Hamiltonian of our system in the interaction picture:

$$\hat{H}_{\rm I} = \hat{V}_{\rm CI} + \hat{V}_{\rm RI}, \tag{1}$$

where

$$\begin{aligned}\hat{V}_{\rm CI} =&\hbar\Omega_1\exp(\mathrm{i}\Delta_1 t)\,|2\rangle\langle 1| \\ &+ \hbar\Omega_2\exp(\mathrm{i}\Delta_2 t)\,|3\rangle\langle 1| \\ &+ \hbar\Omega_3\exp(\mathrm{i}\Delta_3 t)\,|4\rangle\langle 3| \\ &+ \hbar\Omega_4\exp(\mathrm{i}\Delta_4 t)\,|4\rangle\langle 2| + \text{H.c.}, \\ \hat{V}_{\rm RI} =&\hbar\sum_q[g_q^{(1)}a_q\exp(\mathrm{i}\Delta_{1q}t)\,|2\rangle\langle 1| \\ &+ g_q^{(2)}a_q\exp(\mathrm{i}\Delta_{2q}t)\,|3\rangle\langle 1| + \text{H.c.}] \\ &+ \hbar\sum_k[g_k^{(1)}a_k\exp(\mathrm{i}\Delta_{1k}t)\,|4\rangle\langle 3| \\ &+ g_k^{(2)}a_k\exp(\mathrm{i}\Delta_{2k}t)\,|4\rangle\langle 2| + \text{H.c.}].\end{aligned} \tag{2}$$

We define $\Delta_{1,2} = \omega_{2,3} - \omega_1 - \omega_{01}$ and $\Delta_{3,4} = \omega_4 - \omega_{3,2} - \omega_{02}$ as the detunings. $\Omega_{1,2} = \hbar^{-1}E_{01}\boldsymbol{\mu}_{23,1}\cdot\widehat{e}_1$ and $\Omega_{3,4} = \hbar^{-1}E_{02}\boldsymbol{\mu}_{4,32}\cdot\widehat{e}_2$ are Rabi frequencies of the lower and the upper coherent fields, and $E_{01,02}$ and $\hat{e}_{1,2}$ are complex amplitudes and basic vectors of the two coherent fields, respectively. The complex vectors $\hat{\mu}_{23,1} = \langle 2,3| - e\boldsymbol{r}|1\rangle$ and $\hat{\mu}_{4,32} = \langle 4| - e\boldsymbol{r}|3,2\rangle$ correspond to the matrix elements of electronic dipole moments of the transitions from $|2,3\rangle$ to $|1\rangle$ and from $|4\rangle$ to $|2,3\rangle$, respectively. $a_q(a_q^+)$ is the annihilation (creation) operator for the qth vacuum mode which couples the transition from $|2,3\rangle$ to $|1\rangle$ while $a_k(a_k^+)$ is the annihilation (creation) operator for the kth vacuum mode which couples the transition from $|4\rangle$ to $|2,3\rangle$. $\Delta_{1q,2q} = \omega_{2,3} - \omega_1 - \omega_q$and $\Delta_{1k,2k} = \omega_4 - \omega_{3,2} - \omega_k$. $g_q^{(1,2)}$ and $g_k^{(1,2)}$ are the coupling constants between vacuum modes and the atomic transitions.

According to the generalized reservoir theory with the Weisskopf–Wigner approximation[26] and the rotating approximation, we can derive the equations of motion for the reduced atomic density matrix elements as follows:[27,28]

$$\begin{aligned}\dot{\rho}_{44} =& -(r_3+r_4)\rho_{44} - \mathrm{i}\Omega_3\mathrm{e}^{\mathrm{i}t\Delta_3}\rho_{34} - \mathrm{i}\Omega_4\mathrm{e}^{\mathrm{i}t\Delta_4}\rho_{24} \\ &+ \mathrm{i}\Omega_3\mathrm{e}^{-\mathrm{i}t\Delta_3}\rho_{43} + \mathrm{i}\Omega_4\mathrm{e}^{-\mathrm{i}t\Delta_4}\rho_{42},\end{aligned} \tag{3}$$

$$\begin{aligned}\dot{\rho}_{43} =& -\frac{1}{2}(r_2+r_3+r_4)\rho_{43} - \frac{1}{2}p_1\sqrt{r_1r_2}\mathrm{e}^{\mathrm{i}\omega_{23}t}\rho_{42} \\ &+ \mathrm{i}\Omega_2\mathrm{e}^{-\mathrm{i}t\Delta_2}\rho_{41} + \mathrm{i}\Omega_3\mathrm{e}^{\mathrm{i}t\Delta_3}\rho_{44} \\ &- \mathrm{i}\Omega_3\mathrm{e}^{\mathrm{i}t\Delta_3}\rho_{33} - \mathrm{i}\Omega_4\mathrm{e}^{\mathrm{i}t\Delta_4}\rho_{23},\end{aligned} \tag{4}$$

$$\begin{aligned}\dot{\rho}_{42} =& -\frac{1}{2}(r_1+r_3+r_4)\rho_{42} \\ &- \frac{1}{2}p_1\sqrt{r_1r_2}\mathrm{e}^{\mathrm{i}\omega_{32}t}\rho_{43} + \mathrm{i}\Omega_1\mathrm{e}^{-\mathrm{i}t\Delta_1}\rho_{41} \\ &+ \mathrm{i}\Omega_4\mathrm{e}^{\mathrm{i}t\Delta_4}\rho_{44} - \mathrm{i}\Omega_4\mathrm{e}^{\mathrm{i}t\Delta_4}\rho_{22} - \mathrm{i}\Omega_3\mathrm{e}^{\mathrm{i}t\Delta_3}\rho_{32},\end{aligned} \tag{5}$$

$$\begin{aligned}\dot{\rho}_{41} =& -\frac{1}{2}(r_3+r_4)\rho_{41} + \mathrm{i}\Omega_1\mathrm{e}^{\mathrm{i}t\Delta_1}\rho_{42} + \mathrm{i}\Omega_2\mathrm{e}^{\mathrm{i}t\Delta_2}\rho_{43} \\ &- \mathrm{i}\Omega_3\mathrm{e}^{\mathrm{i}t\Delta_3}\rho_{31} - \mathrm{i}\Omega_4\mathrm{e}^{\mathrm{i}t\Delta_4}\rho_{21},\end{aligned} \tag{6}$$

$$\begin{aligned}\dot{\rho}_{33} =& -r_2\rho_{33} + r_3\rho_{44} \\ &- \frac{1}{2}p_1\sqrt{r_1r_2}(\mathrm{e}^{\mathrm{i}\omega_{23}t}\rho_{32} + \mathrm{e}^{\mathrm{i}\omega_{32}t}\rho_{23}) \\ &+ \mathrm{i}\Omega_2\mathrm{e}^{-\mathrm{i}t\Delta_2}\rho_{31} + \mathrm{i}\Omega_3\mathrm{e}^{\mathrm{i}t\Delta_3}\rho_{34} \\ &- \mathrm{i}\Omega_2\mathrm{e}^{\mathrm{i}t\Delta_2}\rho_{13} - \mathrm{i}\Omega_3\mathrm{e}^{-\mathrm{i}t\Delta_3}\rho_{43},\end{aligned} \tag{7}$$

$$\begin{aligned}\dot{\rho}_{32} =& -\frac{1}{2}(r_2+r_1)\rho_{32} - \frac{1}{2}p_1\sqrt{r_1r_2}\mathrm{e}^{\mathrm{i}\omega_{32}t}(\rho_{33}+\rho_{22}) \\ &+ p_2\sqrt{r_3r_4}\mathrm{e}^{\mathrm{i}\omega_{32}t}\rho_{44} - \mathrm{i}\Omega_2\mathrm{e}^{\mathrm{i}t\Delta_2}\rho_{12} \\ &- \mathrm{i}\Omega_3\mathrm{e}^{-\mathrm{i}t\Delta_3}\rho_{42} + \mathrm{i}\Omega_1\mathrm{e}^{-\mathrm{i}t\Delta_1}\rho_{31} \\ &+ \mathrm{i}\Omega_4\mathrm{e}^{\mathrm{i}t\Delta_4}\rho_{34},\end{aligned} \tag{8}$$

$$\begin{aligned}\dot{\rho}_{31} =& -\frac{1}{2}r_2\rho_{31} - \frac{1}{2}p_1\sqrt{r_1r_2}\mathrm{e}^{\mathrm{i}\omega_{32}t}\rho_{21} \\ &+ \mathrm{i}\Omega_1\mathrm{e}^{\mathrm{i}t\Delta_1}\rho_{32} + \mathrm{i}\Omega_2\mathrm{e}^{\mathrm{i}t\Delta_2}\rho_{33} \\ &- \mathrm{i}\Omega_2\mathrm{e}^{\mathrm{i}t\Delta_2}(1-\rho_{22}-\rho_{33}-\rho_{44}) \\ &- \mathrm{i}\Omega_3\mathrm{e}^{-\mathrm{i}t\Delta_3}\rho_{41},\end{aligned} \tag{9}$$

$$\begin{aligned}\dot{\rho}_{22} =& -r_1\rho_{22} + r_4\rho_{44} \\ &- \frac{1}{2}p_1\sqrt{r_1r_2}(\mathrm{e}^{\mathrm{i}\omega_{23}t}\rho_{32} + \mathrm{e}^{\mathrm{i}\omega_{32}t}\rho_{23}) \\ &+ \mathrm{i}\Omega_1\mathrm{e}^{-\mathrm{i}t\Delta_1}\rho_{21} + \mathrm{i}\Omega_4\mathrm{e}^{\mathrm{i}t\Delta_4}\rho_{24} \\ &- \mathrm{i}\Omega_1\mathrm{e}^{\mathrm{i}t\Delta_1}\rho_{12} - \mathrm{i}\Omega_4\mathrm{e}^{-\mathrm{i}t\Delta_4}\rho_{42},\end{aligned} \tag{10}$$

$$\begin{aligned}\dot{\rho}_{21} =& -\frac{1}{2}r_1\rho_{21} - \frac{1}{2}p_1\sqrt{r_1r_2}\mathrm{e}^{\mathrm{i}\omega_{23}t}\rho_{31} \\ &+ \mathrm{i}\Omega_1\mathrm{e}^{\mathrm{i}t\Delta_1}\rho_{22} + \mathrm{i}\Omega_2\mathrm{e}^{\mathrm{i}t\Delta_2}\rho_{23} \\ &- \mathrm{i}\Omega_1\mathrm{e}^{\mathrm{i}t\Delta_1}(1-\rho_{22}-\rho_{33}-\rho_{44}) \\ &- \mathrm{i}\Omega_4\mathrm{e}^{-\mathrm{i}t\Delta_4}\rho_{41},\end{aligned} \tag{11}$$

$$\rho_{11} + \rho_{22} + \rho_{33} + \rho_{44} = 1.$$

Here, $r_i (i = 1, 2, 3, 4)$ are spontaneous emission rates corresponding to the transition from $|2\rangle$ to $|1\rangle$, $|3\rangle$ to $|1\rangle$, $|4\rangle$ to $|3\rangle$ and $|4\rangle$ to $|2\rangle$, respectively. Because both the two couple transition pathways are coupled by the same vacuum mode, there exist two cross terms $\frac{\boldsymbol{\mu}_{31} \cdot \boldsymbol{\mu}_{21} (\omega_{2,3} - \omega_1)^3}{3\pi\varepsilon_0 \hbar c^3}$ and $\frac{\boldsymbol{\mu}_{43} \cdot \boldsymbol{\mu}_{42} (\omega_{2,3} - \omega_1)^3}{3\pi\varepsilon_0 \hbar c^3}$. In the following calculation, we assume $\Delta = \omega_3 - \omega_2$, which is much smaller than $\omega_{2,3} - \omega_1$. Thus, we can replace the cross terms with $p_1\sqrt{r_1 r_2}$ and $p_2\sqrt{r_3 r_4}$ which reflect the magnitude of the quantum interference. The parameter $p_1(p_2)$ is named as alignment of the dipole moment matrix elements $\boldsymbol{\mu}_{31}$ ($\boldsymbol{\mu}_{43}$) and $\boldsymbol{\mu}_{21}$ ($\boldsymbol{\mu}_{42}$), given by $p_1 = \frac{\boldsymbol{\mu}_{31} \cdot \boldsymbol{\mu}_{21}}{|\boldsymbol{\mu}_{31}| \, |\boldsymbol{\mu}_{21}|} \left(p_2 = \frac{\boldsymbol{\mu}_{43} \cdot \boldsymbol{\mu}_{42}}{|\boldsymbol{\mu}_{43}| \, |\boldsymbol{\mu}_{42}|} \right)$. It is clear that as long as $p_1(p_2) \neq 0$, the spontaneous emission rates $r_1(r_3)$ and $r_2(r_4)$ cannot be independent, that is to say, the decay pathways $|2\rangle$-$|1\rangle$ and $|3\rangle$-$|1\rangle$ ($|4\rangle$-$|3\rangle$ and $|4\rangle$-$|2\rangle$) are correlated and interactive. Thus, the decay from $|2\rangle$-$|1\rangle$ ($|4\rangle$-$|3\rangle$) may influence the decay from $|3\rangle$-$|1\rangle$ ($|4\rangle$-$|2\rangle$) of the atom and vice versa. In other words, there exists quantum interference between different pathways. We will discuss in detail the effects of the quantum interference on the absorption and dispersion profile later. Due to the quantum interference, the absorption and the dispersion profile may present very interesting results.

In order to remove the time-dependent factors from Eqs.(3)–(11), we take the following transformation:

$$\begin{aligned}
\Psi_1 &= \rho_{43} \mathrm{e}^{-\mathrm{i}t\Delta_3}; \quad \Psi_2 = \rho_{42} \mathrm{e}^{-\mathrm{i}t\Delta_4}; \\
\Psi_3 &= \rho_{41} \mathrm{e}^{-\mathrm{i}t(\Delta_2+\Delta_3)}; \quad \Psi_4 = \rho_{32} \mathrm{e}^{-\mathrm{i}t\Delta}; \\
\Psi_5 &= \rho_{31} \mathrm{e}^{-\mathrm{i}t\Delta_2}; \quad \Psi_6 = \rho_{44}; \\
\Psi_7 &= \rho_{33}; \quad \Psi_8 = \rho_{22}; \quad \Psi_9 = \rho_{34} \mathrm{e}^{\mathrm{i}t\Delta_3}; \\
\Psi_{10} &= \rho_{24} \mathrm{e}^{\mathrm{i}t\Delta_4}; \quad \Psi_{11} = \rho_{14} \mathrm{e}^{\mathrm{i}t(\Delta_2+\Delta_3)}; \\
\Psi_{12} &= \rho_{23} \mathrm{e}^{\mathrm{i}t\Delta}; \quad \Psi_{13} = \rho_{13} \mathrm{e}^{\mathrm{i}t\Delta_2}; \\
\Psi_{14} &= \rho_{21} \mathrm{e}^{-\mathrm{i}t\Delta_1}; \quad \Psi_{15} = \rho_{12} \mathrm{e}^{\mathrm{i}t\Delta_1}.
\end{aligned} \tag{12}$$

After substituting Eq.(12) for Eqs.(3)–(11), we rewrite these equations in the compact vector form as

$$\frac{\mathrm{d}}{\mathrm{d}t} \hat{\Psi} = \hat{L} \hat{\Psi} + \hat{I}, \tag{13}$$

where $\widehat{\Psi}$ is a column vector whose ith component is Ψ_i; $\widehat{L}$ is a 15×15 matrix, and the inhomogeneous term $\widehat{I}$ is a 15×1 column vector. Hence Eq.(13) has the formal solution

$$\hat{\Psi}(t + \tau) = \mathrm{e}^{\tau \hat{L}} \hat{\Psi}(t) + \hat{L}^{-1} [\mathrm{e}^{\tau \hat{L}} - 1] \hat{I}, \tag{14}$$

and in the steady-state, we have

$$\hat{\Psi}(\infty) = -\hat{L}^{-1} \hat{I}. \tag{15}$$

3. Numerical results

We can numerically calculate absorption and dispersion profiles and population distribution of each level by using the steady-state solution.[15] The absorption and dispersion profiles between $|3\rangle$ and $|1\rangle$ can be obtained by plotting $\mathrm{Im}[\rho_{13}(\infty)]$ and $\mathrm{Re}[\rho_{13}(\infty)]$ versus the detuning Δ_1 (for simplicity, we set $r_1 = r_2 = r_3 = r_4 = r = 1$, and the Rabi frequencies and detunings are scaled by the spontaneous rate r).

3.1. Not taking p_2 into account ($p_2 = 0$)

As the upper coherent field is located at the middle of level $|2\rangle$ and $|3\rangle$, and the lower coherent field conducts a large-scale scanning, i.e. $\Delta = 0.2, \Delta_3 = -0.1, \Delta_4 = 0.1$, it is clear that the absorption profile evolves into a dispersion one gradually, and vice versa. With the increasing of parameter p_1, a dip and a peak occur between the two absorption peaks. Especially when $p_1 = 1$, the absorption profile evolves into dispersion completely and a super-narrow negative absorption peak appears, as shown in Fig.2. Under this condition, the population distribution is $\rho_{11} = 0.375$, $\rho_{22} = 0.323$, $\rho_{33} = 0.300$ and $\rho_{44} = 0.002$. Because $\rho_{11} > \rho_{33}$, this is gain without population inversion. Therefore, quantum interference plays a critical role in the variation of the profiles.

Figure 3 shows the population distribution of each level when $p_1 = 0$ and $p_1 = 1$. The other parameters are the same as in Fig.2. In the case of $p_1 = 0$, the majority of the population stays in the ground level $|1\rangle$. But in the case of $p_1 = 1$, the population distribution becomes completely different. Level $|4\rangle$ is almost empty and the population is all trapped in levels $|1\rangle$, $|2\rangle$ and $|3\rangle$. Corresponding to the variation of the profiles of the absorption and dispersion the population distribution also has a dramatic change when the lower coherent field is tuned to the middle of the two intermediate levels. This gives us the information that quantum interference affects the population distribution and the variation of the profiles is closely related to the population distribution.

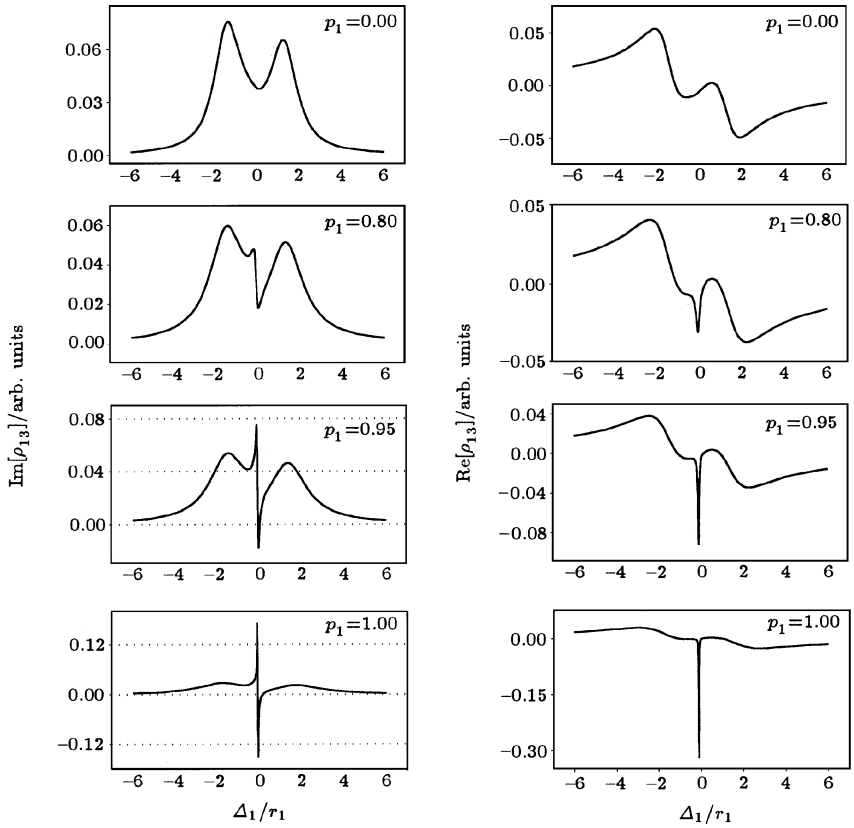


Fig.2. Absorption and dispersion profiles of probing transition from $|3\rangle$ to $|1\rangle$ versus Δ_1 under the condition. $\Delta = 0.2$, $\Delta_2 = \Delta + \Delta_1$, $\Delta_3 = -0.1$, $\Delta_4 = \Delta + \Delta_3$, $\Omega_{1,2} = 0.1$, $\Omega_{3,4} = 1$.

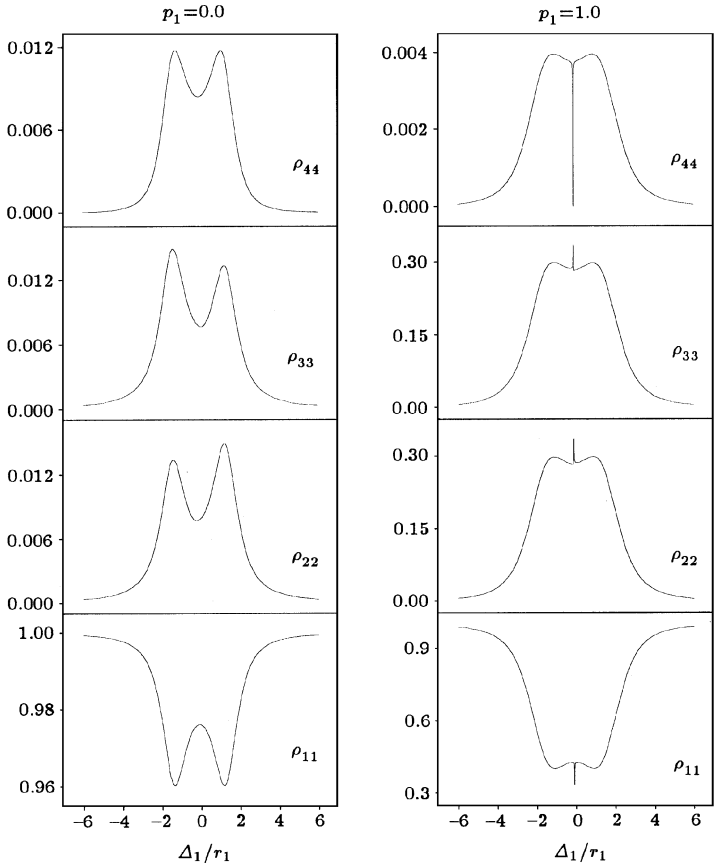


Fig.3. Population of each level versus the detuning Δ_1 under the condition. $\Delta = 0.2$, $\Delta_2 = \Delta + \Delta_1$, $\Delta_3 = -0.1$, $\Delta_4 = \Delta + \Delta_3$, $\Omega_{1,2} = 0.1$, $p_1 = 1$.

Figure 4 shows the variation of absorption profile of $|3\rangle \rightarrow |1\rangle$ with the alteration of the separation between level $|2\rangle$ and $|3\rangle$. When $p_1 = 1$, the greater the separation is, the wider the line-width of the positive absorption peak becomes, but the negative peak drops. If the separation exceeds 8, the gain peak vanishes. The increment of the separation leads to the decrease of the correlation between level $|2\rangle$ and $|3\rangle$. We can derive this conclusion from Eqs.(3)–(11). When Δ is very great, the density matrix elements will oscillate rapidly which can wipe out the correlation between level $|2\rangle$ and $|3\rangle$.

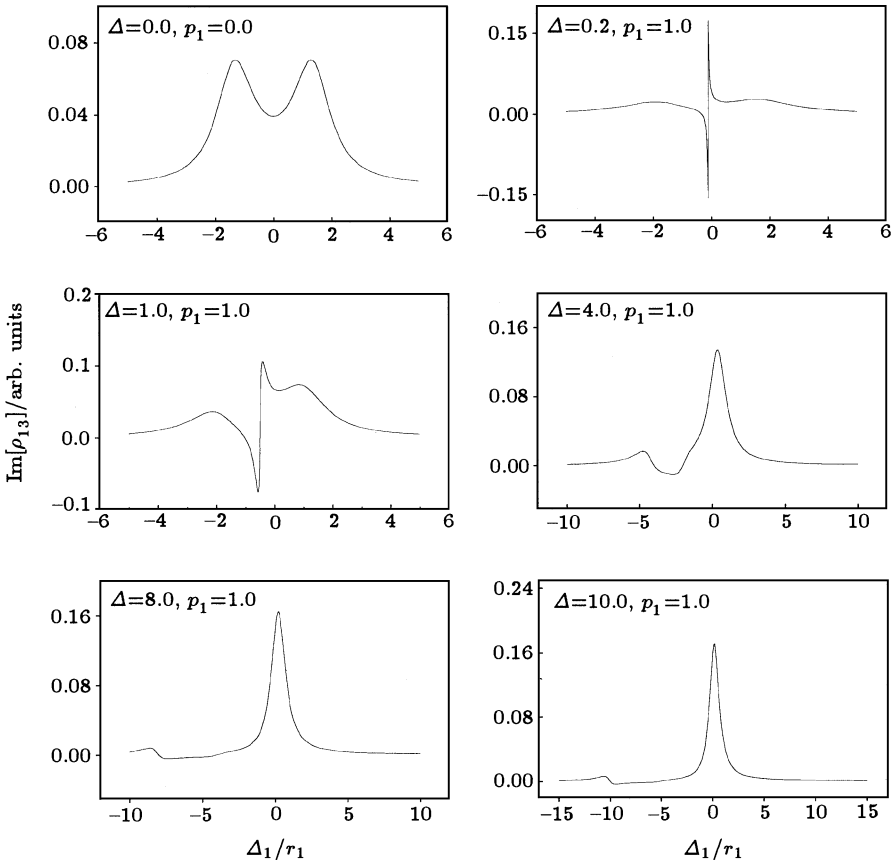


Fig.4. Absorption profiles probing ω_{13} versus the detuning $\Delta_1$with various values of Δ. The parameters are $\Delta_2 = \Delta + \Delta_1$, $\Delta_3 = -0.1$, $\Delta_4 = \Delta + \Delta_3$, $\Omega_{1,2} = 0.1$, $\Omega_{3,4} = 1$.

3.2. Taking p_2 into account ($p_2 \neq 0$)

In the above discussion we do not consider the alignment of the dipole moment matrix elements p_2. From Eqs.(3)–(11), we can clearly see that only Eq.(8) contains p_2. Therefore, we can conclude that the effect of p_2 is related to the population of $|4\rangle$. However, the population of $|4\rangle$ is always small as shown in Fig.3. Figure 5 gives us the profiles of absorption and dispersion, where solid and dotted lines correspond to the situation $p_2 = 0$ and $p_2 = 1$ respectively. When the lower coherent field is tuned to the middle of the two intermediate levels, p_2 has no effect. On both sides of the resonant position, the effect of p_2 is relatively evident. This is related to the population of $|4\rangle$ as shown in Fig.3.

4. Dressed state explanation

Many experimental and theoretical results demonstrate that quantum interference effect is associated with the coherent population trapping. To understand the origin of these numerical results, we analyse the population distribution in the dressed-state representation.

In the rotating frame, the Hamiltonian of the system can be written in the form of

$$\hat{H} = \hat{H}'_b + \hat{V}'_c + \hat{V}'_R, \tag{16}$$

where

$$\begin{aligned}\hat{H}_b' =&\hbar\Delta_1 |2\rangle\langle 2| + \hbar\Delta_2 |3\rangle\langle 3| \\ &+ \hbar(\Delta_2+\Delta_3)|4\rangle\langle 4|, \qquad (17)\\ \hat{V}_c' =&\hbar\Omega_1(|2\rangle\langle 1| + |2\rangle\langle 1|) + \hbar\Omega_2(|1\rangle\langle 3| + |3\rangle\langle 1|) \\ &+ \hbar\Omega_3(|4\rangle\langle 3| + |3\rangle\langle 4|) \\ &+ \hbar\Omega_4(|4\rangle\langle 2| + |2\rangle\langle 4|), \qquad (18)\\ \hat{V}_R' =&\hbar\sum_q \mathrm{e}^{\mathrm{i}(\omega_{01}-\omega_q)t}[g_q^{(1)}a_q|2\rangle\langle 1| \\ &+ g_q^{(2)}a_q|3\rangle\langle 1| + \mathrm{H.c.}] \\ &+ \hbar\sum_k \mathrm{e}^{\mathrm{i}(\omega_{02}-\omega_k)t}[g_k^{(1)}a_k|4\rangle\langle 3| \\ &+ g_k^{(2)}a_k|4\rangle\langle 2| + \mathrm{H.c.}]. \qquad (19)\end{aligned}$$

Now V_c' and $\hat{H}_b'$ are time-independent. The eigenvectors of $\hat{H}_b'$ are the bare atomic state, i.e. $|1\rangle$, $|2\rangle$, $|3\rangle$, $|4\rangle$ define the bare atomic representation. The eigenvectors of $\hat{H}_b' + \hat{V}_c'$ build the atomic dressed-state representation:

$$(\hat{H}_b' + \hat{V}_c')|\varphi_\sigma\rangle = \hbar G_\sigma |\varphi_\sigma\rangle, \qquad (20)$$

where

$$|\varphi_\sigma\rangle = C_{\sigma1}|1\rangle + C_{\sigma2}|2\rangle + C_{\sigma3}|3\rangle + C_{\sigma4}|4\rangle.$$

The matrix form of Eq.(20) can be written as

$$\begin{pmatrix} -\hbar G_\sigma & \hbar\Omega_1 & \hbar\Omega_1 & 0 \\ \hbar\Omega_1 & \hbar\Delta_1 - \hbar G_\sigma & 0 & \hbar\Omega_2 \\ \hbar\Omega_1 & 0 & \hbar\Delta_2 - \hbar G_\sigma & \hbar\Omega_2 \\ 0 & \hbar\Omega_2 & \hbar\Omega_2 & \hbar(\Delta_3+\Delta_2) - \hbar G_\sigma \end{pmatrix} \begin{pmatrix} C_{\sigma1} \\ C_{\sigma2} \\ C_{\sigma3} \\ C_{\sigma4} \end{pmatrix} = 0. \qquad (21)$$

On condition of two-photon resonance, the detunings satisfy $\Delta_1 = -\frac{\Delta}{2}, \Delta_2 = \frac{\Delta}{2}, \Delta_3 = -\frac{\Delta}{2}, \Delta_4 = \frac{\Delta}{2}$. For simplification, we assume that $\Omega_1^* = \Omega_1$, $\Omega_2^* = \Omega_2, \Omega_3^* = \Omega_3, \Omega_4^* = \Omega_4$and $p_2 = 0$. According to Eq.(21), the eigenvalues of the dressed-state can be given as

$$\begin{aligned}G_1 =&G_2 = 0; \\ G_3 =&-\frac{1}{2}\sqrt{\Delta^2 + 8\Omega_1^2 + 8\Omega_2^2}; \\ G_4 =&\frac{1}{2}\sqrt{\Delta^2 + 8\Omega_1^2 + 8\Omega_2^2}. \qquad (22)\end{aligned}$$

We define $G = \sqrt{\Delta^2 + 8\Omega_1^2 + 8\Omega_2^2}$, and the normalized eigenvectors of the dressed-state can be given as

$$|\varphi_1\rangle = -\frac{\Omega_2}{\sqrt{\Omega_1^2+\Omega_2^2}}|1\rangle + \frac{\Omega_1}{\sqrt{\Omega_1^2+\Omega_2^2}}|4\rangle; \qquad (23a)$$

$$\begin{aligned}|\varphi_2\rangle =& -\frac{\Delta}{\sqrt{8\Omega_1^2+\Delta^2}}|1\rangle - \frac{2\Omega_1}{\sqrt{8\Omega_1^2+\Delta^2}}|2\rangle \\ &+ \frac{2\Omega_1}{\sqrt{8\Omega_1^2+\Delta^2}}|3\rangle; \qquad (23b)\end{aligned}$$

$$|\varphi_3\rangle = \frac{2\Omega_1}{G}|1\rangle - \frac{\Delta+G}{2G}|2\rangle + \frac{\Delta-G}{2G}|3\rangle + \frac{2\Omega_2}{G}|4\rangle; \qquad (23c)$$

$$|\varphi_4\rangle = \frac{2\Omega_1}{G}|1\rangle - \frac{\Delta-G}{2G}|2\rangle + \frac{\Delta+G}{2G}|3\rangle + \frac{2\Omega_2}{G}|4\rangle. \qquad (23d)$$

In this basis, we can numerically calculate the population distribution of each dressed level ($\rho_{\varphi_{11}}$, $\rho_{\varphi_{22}}$, $\rho_{\varphi_{33}}$, $\rho_{\varphi_{44}}$) as shown in Fig.6. Corresponding to $p_1 = 1$, population is trapped in the dressed state $|\varphi_2\rangle$ thoroughly which is similar to the results that Zhou and Swain[23] and Li *et al*[25] realized in the V-type and quasi-V-type four-level system. Whether two dipole moments are parallel or not obviously plays an important role in quantum interference processes. On the other hand, the dressed state $|\varphi_2\rangle$ is the superposition of bare atomic states $|1\rangle$, $|2\rangle$ and $|3\rangle$, so the population trapping effect is independent of $|4\rangle$. In addition, when $\Delta_1 = -\Delta_2 = \Delta_3 = -\Delta_4 = -\frac{\Delta}{2}$ and $p_1 = 1$, the absorption and dispersion profiles have nothing to do with the upper coherent field and p_2, which is shown in Fig.5.

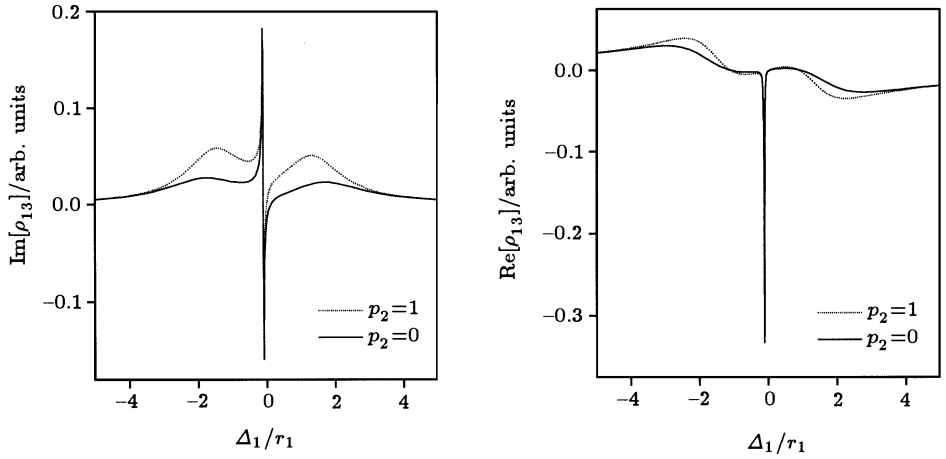


Fig.5. Absorption and dispersion profiles, solid lines corresponding to $p_2 = 0$ and dotted lines corresponding to $p_2 = 1$.

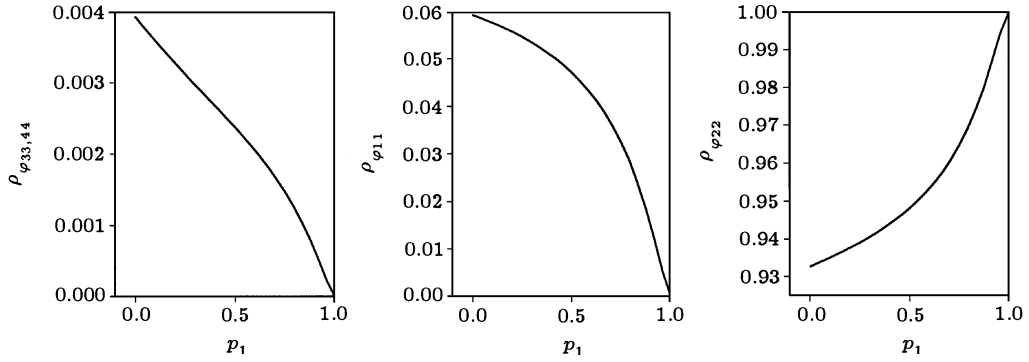


Fig.6. Population distribution of each dressed-level ($\rho_{\varphi 11}$, $\rho_{\varphi 22}$, $\rho_{\varphi 33}$, $\rho_{\varphi 44}$) versus the values of p under the condition $\Delta = 0.2$, $\Delta_2 = \Delta + \Delta_1$, $\Delta_3 = -0.1$, $\Delta_4 = \Delta + \Delta_3$, $\Omega_{1,2} = 0.1$, $p_2 = 0$.

5. Conclusion

This paper has discussed the variation of the absorption and dispersion profiles and the population distributions of each level. We find in theory that the correlation between two dipole moments $\boldsymbol{\mu}_{21}$, $\boldsymbol{\mu}_{31}$, and $\boldsymbol{\mu}_{43}$, $\boldsymbol{\mu}_{42}$ (which indicate the magnitude of quantum interference between the different spontaneous emission pathways, respectively) play a very important role in the variation process. If the two coherent fields are two-photon resonant with $|4\rangle - |1\rangle$, and simultaneously p_1=1, the amplitude of the upper coherent field and p_2 do not affect the profiles and the population distribution. Contrarily, the effect of the upper driving field and p_2 cannot be neglected. The magnitude of the separation of two intermediate levels also influences the absorption and dispersion profiles when other parameters are fixed. In the dressed-state representation, the population distribution of the dressed-state exhibits a coherent population trapping which is the origin of the previous results in the two-photon resonant excitation ladder-system.

References

[1] Harris S E 1989 *Phys. Rev. Lett.* **62** 1033
[2] Kocharovskaya O and Khanin Ya A 1988 *JETP Lett.* **48** 630
[3] Agarwal G S 1991 *Phys. Rev.* A **44** R28
[4] Zhu S Y, Narducci L M and Scully M O 1995 *Phys. Rev.* A **52** 4791
[5] Agarwal G S 1991 *Phys. Rev. Lett.* **67** 980
[6] Scully M O, Zhu S Y and Favrielides A 1989 *Phys. Rev.* A **62** 2813
[7] Kocharovskaya O and Mandel P 1990 *Phys. Rev.* A **42** 523
[8] Scully M O 1991 *Phys. Rev. Lett.* **67** 1855
[9] Scully M O and Zhu S Y 1992 *Opt. Commun.* **87** 134
[10] Zibrov A S *et al* 1996 *Phys. Rev. Lett.* **76** 3935
[11] Li F L and Zhu S Y 1999 *Phys. Rev.* A **59** 2330
[12] Zhu S Y and Scully M O 1996 *Phys. Rev. Lett.* **76** 388

[13] Hegerfeladt G C and Plenio M B 1992 *Phys. Rev. Lett.* **46** 373
[14] Imamoglu A and Harris S E 1989 *Opt. Lett.* **66** 1033
[15] Hioe F T and Eberly J H 1981 *Phys. Rev. Lett.* **47** 838
[16] Hioe F T 1983 *Phys. Rev.* A **28** 879
[17] Hioe F T 1984 *Phys. Rev.* A **30** 3097
[18] Smirnov V S, Tumaikin A M and Yudin V I 1989 *Sov. Phys. JEPT* **69** 913
[19] Hakuta K, Marmet L and Stoiche B P 1991 *Phys. Rev. Lett.* **66** 596
[20] Fulton D J, Shepherd S, Mosley R R, Sinclair B D and Dunn M H 1995 *Phys. Rev.* A **52** 2302
[21] Zhou P and Swain S 1997 *Phys. Rev. Lett.* **78** 832
[22] Zhou P and Swain S 1996 *Phys. Rev. Lett.* **77** 3995
[23] Zhou P and Swain S 1997 *Phys. Rev.* A **56** 3011
[24] Narducci L M and Scully M O 1990 *Phys. Rev.* A **42** 1630
[25] Li F L, Zhu S Y and Ma A Q 2001 *J. Mod. Opt.* **48** 439
[26] Sargent M III, Scully M O and Lamb W E Jr. 1974 *Laser Physics* (Addison-Wesley, Reading, MA) Chap. 16 p273
[27] Fleischhauer M *et al* 1992 *Opt. Commun.* **94** 599
[28] Lax M 1963 *Phys. Rev.* **129** 2342